JOURNAL OF MATERIALS SCIENCE **39** (2004) 107–112

Study on the interaction between a dislocation and impurities in KCl:Sr^{2+} single crystals by the Blaha effect

Part III *Influence of heat treatment on various characteristics*

Y. KOHZUKI, T. OHGAKU
Faculty of Engineering, Kanazawa University, Kodatsuno 2-40-20, Kanazawa 920-8667, Japan

Strain-rate cycling tests associated with ultrasonic oscillation were conducted at 80–239 K for two kinds of KCl:Sr^{2+} (0.05 mol% in the melt) single crystals: quenched and annealed specimens. Examining the relationship of temperature and dislocation velocity-effective stress exponent, m^*, estimated from the data obtained in this series, we could find the suitable force-distance relation between a dislocation and the impurity. The force-distance relation for the quenched specimen approached to the Fleischer's model taking account of the Friedel relation rather than the Fleischer's model. As for the annealed specimen, the SQ was the most appropriate of the three models: the SQ, the PA, and the TR indicate a square, a parabolic, and a triangular force-distance profile respectively. The three force-distance relations are taken account of the Friedel relation. By annealing the quenched specimen, m^* became low at a given temperature. This may have been caused by the following two phenomena. First, the concentration of weak obstacles to dislocation motion decreased after the heat treatment. Secondly, the resistance to movement of a dislocation in the quenched specimen was weakened by annealing it, e.g., F_0 was reduced to about one-third and φ_0 increased from 154 to 172 degrees. F_0 and φ_0 are the force acted on the dislocation and the bending angle of dislocation by the weak obstacle such as the impurity. Therefore, it may be deduced that the dislocation velocity in the quenched specimen is more sensitive to the effective stress due to the impurities than that in the annealed specimen at the temperature. © *2004 Kluwer Academic Publishers*

1. Introduction

When alkali halide crystals are doped with divalent ions, the ions are expected to be paired with positive ion vacancies. The pairs are termed I–V dipoles. If the I–V dipoles in KCl:Sr^{2+} single crystals aggregate by heat treatment, various deformation characteristics will be changed. This is because the state of a small amount of impurities in the crystals strongly influences the resistance to movement of a dislocation [1]. In part II [2] of this series, the influence of the heat treatment on the force-distance relation between a dislocation and the impurity was described from the dependence of strain-rate sensitivity due to the impurities on temperature. In part III, the study is carried out in more detail by examining the relation between temperature and dislocation velocity-effective stress exponent, m^*, expressed by [3]

$$v = A\tau^{m^*} \tag{1}$$

where v is the average velocity of dislocation, τ is the effective shear stress, and A and also m^* are constants for a given material and temperature. Although Equation 1 is regarded as an empirical relationship [4], m^* is useful for investigating the behavior of thermally activated dislocation motion in various materials (e.g., NaCl contained Ca^{2+}, Mg^{2+}, Sr^{2+}, and Ba^{2+} [5], body-centered cubic metals [6], Nb [7], LiF:Mg^{2+} [8], and binary iron-base alloys contained Co, Cr, Al, Si, Ni and Mn, respectively [9]). In addition, the influence of a state of the impurities on the deformation characteristics (i.e., the force acted on the dislocation and the bending angle of dislocation by the impurity) is investigated on the basis of the data obtained in this series.

2. Experimental procedure

Two kinds of KCl:Sr^{2+} (0.05 mol% in the melt) single crystals, which were about $5 \times 5 \times 15$ mm^3, were deformed at 80–240 K by compression along the ⟨100⟩ axis and ultrasonic oscillatory stress was applied by a resonator in the same direction as the compression during a strain-rate cycling test. Specimens were prepared by the following treatment. The specimens were cooled to room temperature at a rate of 40 Kh^{-1} after keeping at 973 K for 24 h in order to reduce dislocation density. Further, the specimens were held at 673 K for

30 min and were cooled by water quenching in order to disperse the impurities immediately before the test. These specimens are termed the quenched specimens in this paper. The other kind of specimens were obtained by keeping the quenched specimens at 370 K for 500 h and gradually cooling in a furnace for the purpose of aggregating the impurities [10]. These are termed the annealed specimens in this paper. The strain-rate cycling test associated with the oscillation has been described in the previous papers [11–13].

3. Results and discussion

3.1. Force-distance relation between a dislocation and the impurity

3.1.1. Quenched specimen

Deformation behavior has been investigated with the $m_{\varepsilon=0}$ which is obtained by extrapolating a relative curve of strain-rate sensitivity, $\Delta\ln\dot{\varepsilon}/\Delta\ln\tau_a$, and shear strain to zero strain [14–18]. $\Delta\ln\tau_a$ is the logarithmic change in applied shear stress due to the strain-rate cycling test without the oscillation during plastic deformation. The value of $m_{\varepsilon=0}$ for alkali halide was considered to be m^* [19] (i.e., the values of m^* are about 26.5 for the quenched specimen at 175 K and 20.0 for the annealed specimen at 125 K, as can be seen from Fig. 1a and b). Using $m_{\varepsilon=0}$, reasonable value of effective stress and hardening mechanism were found for zone-refined iron [15] and potassium contained Na^+ (25 p.p.m.) [16] during the deformation. Open circles in Fig. 2 correspond to the $m_{\varepsilon=0}$ for the quenched specimen.

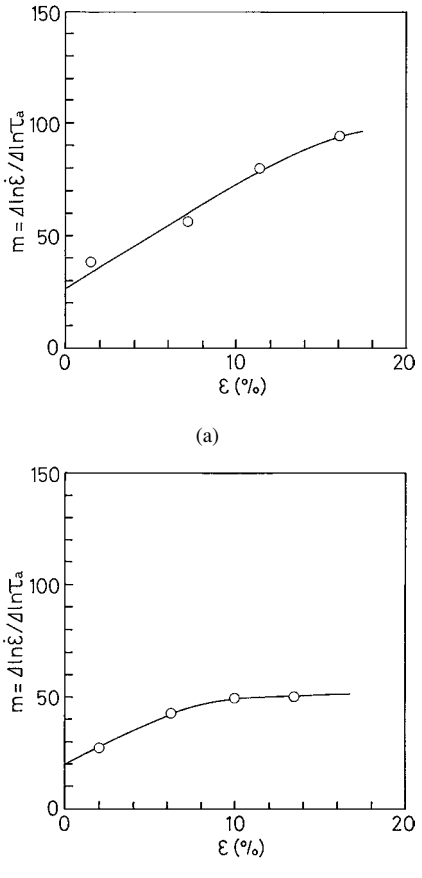

Figure 1 Variation of m with shear strain for (a) the quenched specimen at 175 K and (b) the annealed specimen at 125 K.

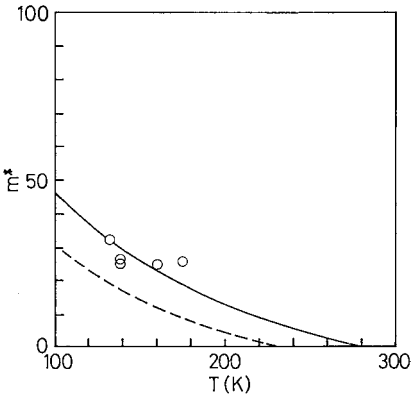

Figure 2 Relationship between the temperature and the dislocation velocity-effective stress exponent for the quenched specimen at the two models: (---) the Fleischer's model and (—) the F-F. Open circles represent the $m_{\varepsilon=0}$ for the quenched specimen.

The m^* for the Fleischer's model was given by [20] as:

$$m^* = F_0 b\{(\tau/\tau_0)^{1/2} - (\tau/\tau_0)\}/(kT) \qquad (2)$$

where F_0 is the force acted on the dislocation at 0 K, b is the magnitude of the Burgers vector, τ_0 is the effective shear stress τ at 0 K, and kT has the usual meaning. The Fleischer's model has been widely used for the interaction between a dislocation and an impurity in ionic crystals doped with divalent cations [20–23]. The temperature dependence of the effective stress was given by [20]

$$(\tau/\tau_0)^{1/2} = 1 - (T/T_c)^{1/2} \qquad (3)$$

where T_c is the critical temperature at which the effective stress is zero. Combining Equations 2 and 3, we can evaluate the m^* for the Fleischer's model as follows

$$m^* = F_0 b\{(T_c/T)^{1/2} - 1\}/(kT_c) \qquad (4)$$

Friedel [24] derived an expression for the average spacing of weak obstacles along the dislocation. The m^* for the Fleischer's model taking account of the Friedel relation, which is abbreviated as F-F in this paper, can be obtained from the equation:

$$m^* = 2F_0 b\{(T_c/T)^{1/2} - 1\}/(3\,kT_c) \qquad (5)$$

The development of Equation 5 is described in [25]. The results of Equations 4 and 5, in which F_0 and T_c are given in Table I, are represented as a dashed and a

TABLE I Values of F_0 and T_c for various force-distance relations between a dislocation and the impurity in the two specimens

Specimen	Force-distance relation	F_0 ($\times 10^{-10}$ N)	T_c (K)
Quenched specimen	Fleischer	5.25	227 [12]
	F-F	9.20	289 [32]
Annealed specimen	SQ	2.85	220 [2]
	PA	3.75	225 [2]
	TR	4.65	228 [2]

TABLE II Values of τ_{p0} for various force-distance relations between a dislocation and the impurity in the two specimens

Specimen	Force-distance relation	τ_{p0} (MPa)
Quenched specimen	Fleischer	14.52 [12]
	F-F	25.47 [32]
Annealed specimen	SQ	2.17 [2]
	PA	3.28 [2]
	TR	4.53 [2]

solid line respectively in Fig. 2. The value of F_0 for the Fleischer's model is calculated from

$$F_0 = \tau_{p0} L b \tag{6}$$

and that for the F-F from

$$F_0 = \tau_{p0}\, b\left\{2L_0^2 E \big/ (\tau_{p0}\, b)\right\}^{1/3} \tag{7}$$

where τ_{p0} is the effective shear stress due to the impurities without thermal activation [12, 26, 27], L is the average spacing of impurities along the dislocation, L_0 is the average spacing of impurities on the slip plane, and E is the line tension of the dislocations. τ_{p0} is given in Table II. The value of T_c in Equation 4 is obtained from Fig. 3a and that in Equation 5 from Fig. 3b. The relation between (τ_{p1}/τ_{p0}) and temperature is considered to reveal the force-distance relation between a dislocation and an impurity, because τ_{p1} corresponds to the effective stress due to only one type of the impurities which lie on the dislocation when the dislocation moves forward with the help of oscillation [12, 26, 27].

The open circles are fitted to the solid line in comparison with the dashed line as shown in Fig. 2. Therefore, the force-distance relation for the quenched specimen is suited to the F-F rather than the Fleischer's model at the temperature. Even though the open circles are given within the narrow range of temperature, this method is useful for the determination of suitable model.

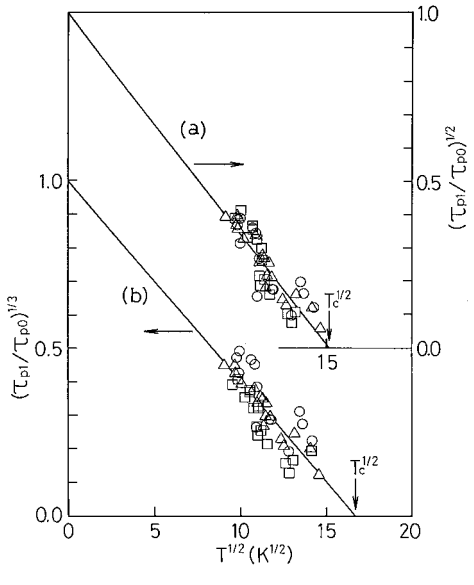

Figure 3 Linear plots of the effective shear stress and the temperature at (a) the Fleischer's model and (b) the F-F for the quenched specimen: KCl:Sr^{2+} ((○) 0.035 mol%, (△) 0.050 mol%, (□) 0.065 mol% in the melt).

3.1.2. Annealed specimen

It was clear that the force-distance relation for the annealed specimen could not be approximated by the Fleischer's model and the F-F [2, 28], whereas the other models were not distinct [2]. We investigate the applicability of three models [29]: a square, a parabolic, and a triangular force-distance relation, which are termed the SQ, the PA, and the TR respectively in this paper. The three force-distance relations are taken into account the Friedel relation [24].

When the thermally activated overcoming of the aggregates controls the dislocation velocity and the dislocation moves forward the distance of L_0^2/L, the dislocation velocity is given by

$$v = \nu\left(L_0^2/L\right)\exp\{-\Delta G/(kT)\} \tag{8}$$

where ν is the frequency of vibration of a dislocation segment, ΔG is the change in Gibbs free energy of activation for the dislocation motion. The Gibbs free energy for the SQ is given by [2]

$$\Delta G = \Delta G_0 - \beta\tau^{2/3} \tag{9}$$

$$\beta = \left(2\mu b^4 d^3 L_0^2\right)^{1/3} \tag{10}$$

where μ is the shear modulus and d is an activation distance. The PA gives [2]

$$\Delta G = \Delta G_0\{1 - (\tau/\tau_0)^{2/3}\}^{3/2} \tag{11}$$

and the TR gives [2]

$$\Delta G = (\beta/8)\left(\tau_0^{2/3} - 2\tau^{2/3} + \tau_0^{-2/3}\tau^{4/3}\right) \tag{12}$$

Combining Equation 10 and the Friedel relation:

$$L = \left\{2L_0^2 E \big/ (\tau_0\, b)\right\}^{1/3} \tag{13}$$

the β is expressed by

$$\beta = \tau_0^{1/3} L b d = \Delta G_0 \tau_0^{-2/3} \tag{14}$$

Substituting Equation 14 into Equations 9 and 12, we find

$$\Delta G = \Delta G_0\{1 - (\tau/\tau_0)^{2/3}\} \tag{15}$$

$$\Delta G = (\Delta G_0/8)\{1 - 2(\tau/\tau_0)^{2/3} + (\tau/\tau_0)^{4/3}\} \tag{16}$$

From Equations 8 and 15, the dislocation velocity for the SQ is expressed by

$$v = \nu\left(L_0^2/L\right)\exp[-F_0 b\{1 - (\tau/\tau_0)^{2/3}\}/(kT)] \tag{17}$$

From Equations 8 and 11, that for the PA yields

$$v = \nu\left(L_0^2/L\right)\exp[-F_0 b\{1 - (\tau/\tau_0)^{2/3}\}^{3/2}/(kT)] \tag{18}$$

Similarly from Equations 8 and 16, that for the TR is

$$v = \nu\left(L_0^2/L\right)\exp[-F_0 b\{1 - 2(\tau/\tau_0)^{2/3} + (\tau/\tau_0)^{4/3}\}/(8kT)] \quad (19)$$

It is well known that m^* can be obtained from the following equation:

$$m^* = \partial \ln v/\partial \ln \tau = \tau(\partial \ln v/\partial \tau) \quad (20)$$

$(\partial \ln v/\partial \tau)$ in Equation 20 can be found from Equation 17 as follows

$$\partial \ln v/\partial \tau = \{2F_0 b/(3kT\tau_0)\}(\tau/\tau_0)^{-1/3} \quad (21)$$

From Equation 18, we can find

$$\partial \ln v/\partial \tau = \{F_0 b/(kT\tau_0)\}\{1 - (\tau/\tau_0)^{2/3}\}^{1/2}(\tau/\tau_0)^{-1/3} \quad (22)$$

Similarly from Equation 19, we obtain

$$\partial \ln v/\partial \tau = \{F_0 b/(6kT\tau_0)\}\{(\tau/\tau_0)^{-1/3} - (\tau/\tau_0)^{1/3}\} \quad (23)$$

Therefore, m^* for the SQ is expressed by

$$m^* = \{2F_0 b/(3kT)\}(\tau/\tau_0)^{2/3} \quad (24)$$

The formula relating the effective stress and temperature for the SQ is

$$(\tau/\tau_0)^{2/3} = 1 - (T/T_c) \quad (25)$$

For PA the equivalent expression is

$$(\tau/\tau_0)^{2/3} = 1 - (T/T_c)^{2/3} \quad (26)$$

and for TR

$$(\tau/\tau_0)^{2/3} = 1 - (T/T_c)^{1/2} \quad (27)$$

Substituting Equation 25 into Equation 24, m^* for the SQ can be obtained as follows

$$m^* = \{2F_0 b/(3k)\}\left(T^{-1} - T_c^{-1}\right) \quad (28)$$

In the same way, m^* for the PA from Equations 20, 22, and 26 is expressed by

$$m^* = \{F_0 b/(kT)\}\{(T/T_c)^{1/3} - (T/T_c)\} \quad (29)$$

and using Equations 20, 23, and 27, m^* for the TR is

$$m^* = \{F_0 b/(6kT)\}\{(T/T_c)^{1/2} - (T/T_c)\} \quad (30)$$

Each curve in Fig. 4 for the annealed specimen corresponds to the relation between temperature and m^* derived from Equation 28 for the SQ, Equation 29 for the PA, and Equation 30 for the TR. F_0 for the three models is calculated from Equation 7 in which the value of τ_{p0} is given in Table II. F_0 and T_c are tabulated in Table I. The relative curve of temperature and the m^* for the SQ, that for the PA, and that for the TR are represented as a solid line, a dashed line, and a dash-dotted line in Fig. 4. Open circles correspond to the m^* for the annealed specimen, which are obtained from $m_{\varepsilon=0}$. Unfortunately, it was difficult to evaluate m^* above around 180 K, because the error in the measurement of $m_{\varepsilon=0}$ is large. As can be seen from Fig. 4, the open circles increase with decreasing temperature and approach to the solid line of SQ. Accordingly, it is considered that the SQ can be selected as the most suitable force-distance relation among the three.

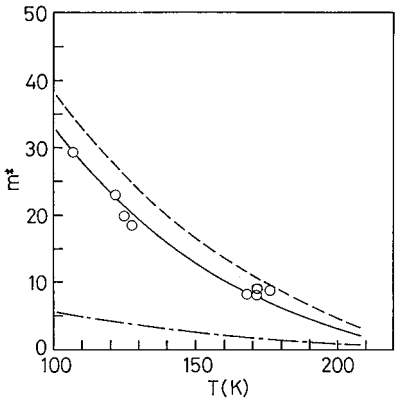

Figure 4 Relationship between the temperature and the dislocation velocity-effective stress exponent for the annealed specimen at the three models: (---) the PA, (—) the SQ, and (–·–) the TR. Open circles represent the $m_{\varepsilon=0}$ for the annealed specimen.

3.2. F_0, L/L_0, and φ_0

By using Equation 7, F_0 was provided in the preceding section. Then, the line tension of the dislocations is calculated by μb^2. The shear modulus is assumed to be 1.01×10^{10} Pa for [110] direction at 0 K [30]. Further, the average spacing of isolated I–V dipoles on the slip plane may be given by [20, 31]

$$L_0 = b/(4c_1/3)^{1/2} \quad (31)$$

where the concentration of the impurities, c_1, is 98.3 ppm from dielectric loss measurement. The average spacing of the aggregates on the slip plane is given by

$$L_0 = b/c_2^{1/2} \quad (32)$$

where the concentration of the aggregates, c_2, is 32.1 ppm from atomic absorption method, because the aggregates in the annealed specimen are assumed to form the trimers which are arranged hexagonally head to tail in a (111) planes [10]. As a result, F_0 calculated from Equation 7 are 9.20×10^{-10} N and 2.85×10^{-10} N for the quenched and annealed specimens respectively. Thus F_0 is reduced to about one-third by the heat treatment. In addition, the average spacing, L, of impurities along the dislocation at 0 K is 812 Å for the quenched specimen and 2947 Å for the annealed specimen on

TABLE III Values of various characteristics[a] for the two specimens

Specimen	F_0 ($\times 10^{-10}$ N)	L_0 (Å)	L/L_0	φ_0 (degrees)
Quenched specimen	9.20	389	2.1	154 [32]
Annealed specimen	2.85	786	3.8	172

[a]The interaction between a dislocation and the impurity in the quenched specimen is approximated by the F-F and that in the annealed specimen by the SQ.

a calculation from the values of F_0 and τ_{p0}. For the quenched specimen L is about twice as long as L_0, but for the annealed specimen it is quadruple the value of L_0. Therefore, the bending angle, φ_0, at which the dislocation embraces the aggregates under the τ_{p0} is expected to be larger than that for the quenched specimen. We further examine φ_0 for both the specimens. From the equation [32]:

$$\varphi_0/2 = \cos^{-1}\{\tau_{p0}L_0b/(2E)\}^{2/3} \tag{33}$$

φ_0 for the quenched specimen was 154 degrees [32] and that for the annealed specimen 172 degrees. The various characteristics are summarized in Table III. Consequently, the interaction between a dislocation and the impurity for the quenched specimen is stronger in comparison with that for the annealed specimen.

3.3. Influence of heat treatment on m^*

3.3.1. Based on $m_{\varepsilon=0}$

As described in the Section 3.2. of this paper, F_0 decreases and φ_0 increases on annealing of the quenched specimen. Therefore, the resistance of obstacle to the dislocation movement in the quenched specimen is weakened by annealing it. In addition, L_0 becomes large after the heat treatment. That is, the concentration of weak obstacles such as impurities decreases after the treatment. If the results for F_0, L/L_0, φ_0, and L_0 are real, it is expected that the value of m^* for KCl:Sr^{2+} becomes smaller by the heat treatment as, according to the description [33], m^* becomes smaller when the concentration or the resistance of obstacle to dislocation motion decreases. Fig. 5 shows the m^* for the two kinds of specimens. Open triangles and circles correspond to $m_{\varepsilon=0}$ for the quenched specimen and for the annealed specimen, obtained in the Section 3.1. Dashed and solid lines are derived from Equations 5 and 28. It is clear that the m^* for the annealed specimen is less than that for the quenched specimen at a given temperature, thus proving the above-mentioned prediction, i.e., m^* decreases by the heat treatment. The difference between the values of m^* for the two specimens is 13 to 17 within the temperature range. Fig. 5 also suggests that the dislocation velocity in the quenched specimen is more sensitive to the effective stress due to the obstacles than that in the annealed specimen.

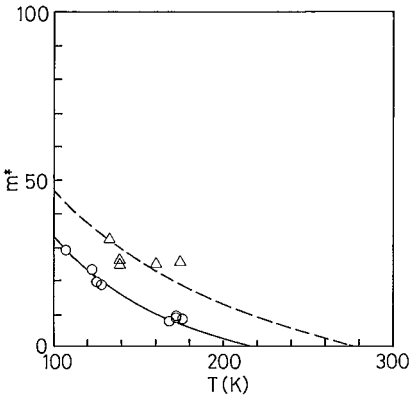

Figure 5 Temperature dependence of the dislocation velocity-effective stress exponent for the two specimens: (△) the quenched specimen and (○) the annealed specimen. Open symbols represent $m_{\varepsilon=0}$. (---) and (—) are calculated by Equations 5 and 28, respectively.

3.3.2. Based on the relation between SRS and $\Delta\tau$

We deduce the values of m^* from the relative curve of strain-rate sensitivity (SRS) and stress decrement ($\Delta\tau$) due to the oscillation. The curve has two bending points and two plateau places and SRS decreases with $\Delta\tau$ between the two bending points [12]. Fig. 6 shows the typical variation of SRS with $\Delta\tau$. The curve was considered to represent the influence of ultrasonic oscillation on the dislocation motion on the slip plane containing many weak obstacles such as impurities and a few strong ones such as forest dislocations [12, 26, 27]. $(\Delta \ln\dot{\varepsilon}/\Delta\tau')_p$, which is given by the difference between SRS at first plateau place and at second one on the relative curve of SRS and $\Delta\tau$, was assumed to be the SRS due to impurities when the dislocation moves forward with the help of oscillation [13, 26, 34]. $\Delta\tau'$ is the stress change due to the strain-rate cycling when the strain-rate cycling associated with the oscillation is carried out keeping the stress amplitude constant. Then, m^* may be expressed by

$$m^* = \tau_{p1}(\Delta \ln\dot{\varepsilon}/\Delta\tau')_p \tag{34}$$

where m^* is examined on the assumption that Equation 20 is also valid for the case of applying the ultrasonic oscillatory stress during plastic deformation. The results of Equation 34 are indicated by open symbols in Fig. 7. Two curves in the figure are to guide the reader's eye. The values of $\tau_{p1}(\Delta \ln\dot{\varepsilon}/\Delta\tau')_p$ tend to

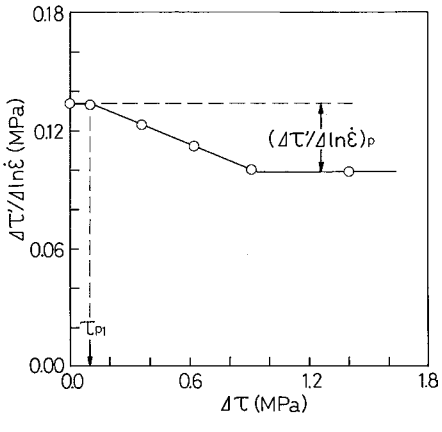

Figure 6 Relationship between the strain-rate sensitivity and the stress decrement for the annealed specimen at 201 K and $\varepsilon = 18\%$.

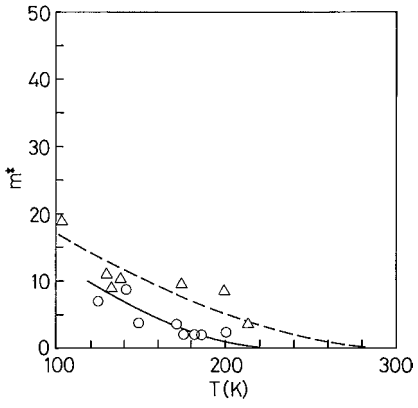

Figure 7 Temperature dependence of the dislocation velocity-effective stress exponent for the two specimens: (△) the quenched specimen and (○) the annealed specimen. Open symbols represent m^* evaluated by $\tau_{p1}(\Delta \ln \dot{\varepsilon}/\Delta\tau')_p$.

increase with decreasing temperature as well as $m_{\varepsilon=0}$ shown in Fig. 5. Furthermore, $\tau_{p1}(\Delta \ln \dot{\varepsilon}/\Delta\tau')_p$ for the annealed specimen is less than that for the quenched specimen at a given temperature. This is also similar to the above observations of $m_{\varepsilon=0}$ for the two specimens.

4. Conclusions

1. On the basis of m^* obtained by $m_{\varepsilon=0}$, the following can be found through Equations 4, 5, and 28–30 at the temperature. The force-distance relation between a dislocation and the impurity in the quenched specimen is approximated by the F-F rather than the Fleischer's model as observed in Fig. 2. As for the annealed specimen, the SQ is the most appropriate among the SQ, PA, and TR models as demonstrated in Fig. 4. In spite of the narrow range of temperature, this method is useful for the determination of suitable force-distance relation.

2. The resistance of weak obstacle to the dislocation movement in the quenched specimen is weakened by annealing it (e.g., F_0 is reduced to about one-third and φ_0 increases from 154 to 172 degrees). Furthermore, the concentration of weak obstacles decreases after the heat treatment. These may lead to the results that m^* calculated by $m_{\varepsilon=0}$ (Fig. 5) or by $\tau_{p1}(\Delta \ln \dot{\varepsilon}/\Delta\tau')_p$ (Fig. 7) at a given temperature is lowered by the heat treatment. From these figures, it may be deduced that the dislocation velocity in the quenched specimen is more sensitive to the effective stress than that in the annealed specimen within the temperature range.

References

1. J. S. DRYDEN, S. MORIMOTO and J. S. COOK, *Philos. Mag.* **12** (1965) 379.
2. Y. KOHZUKI and T. OHGAKU, *J. Mater. Sci.* **36** (2001) 923.
3. W. G. JOHNSTON and J. J. GILMAN, *J. Appl. Phys.* **30** (1959) 129.
4. J. W. CHRISTIAN, *Acta Metall.* **12** (1964) 99.
5. M. T. SPRACKLING, *Philos. Mag.* **27** (1973) 265.
6. M. ANGLADA and F. GUIU, *Scripta Metall.* **13** (1979) 103.
7. F. GUIU and M. ANGLADA, *Philos. Mag.* **46** (1982) 881.
8. J. A. GORRI, A. PAZ and F. GUIU, *Phys. Status Solidi* (a) **82** (1984) 85.
9. K. OKAZAKI, *J. Mater. Sci.* **31** (1996) 1087.
10. J. S. COOK and J. S. DRYDEN, *Proc. Phys. Soc.* **80** (1962) 479.
11. T. OHGAKU and N. TAKEUCHI, *Phys. Status Solidi* (a) **102** (1987) 293.
12. Y. KOHZUKI, T. OHGAKU and N. TAKEUCHI, *J. Mater. Sci.* **28** (1993) 3612.
13. Y. KOHZUKI, *ibid.* **33** (1998) 5613.
14. A. G. EVANS and P. L. PRATT, *Philos. Mag.* **21** (1970) 951.
15. J. T. MICHALAK, *Acta Metall.* **13** (1965) 213.
16. I. M. BERNSTEIN, J. C. M. LI and M. GENSAMER, *ibid.* **15** (1967) 801.
17. K. S. LEE and W. K. PARK, *J. Kor. Nucl. Soc.* **10** (1978) 73.
18. N. TAKEUCHI, K. TERADA and S. YONETANI, *Zairyo* **27** (1978) 176 (in Japanese).
19. T. IMURA, in "Strength of Crystals," edited by R. R. Hasiguti and S. Chikazumi (Asakurashoten, Tokyo, 1968) p. 28 (in Japanese).
20. R. L. FLEISCHER, *J. Appl. Phys.* **33** (1962) 3504.
21. R. L. FLEISCHER and W. R. HIBBARD, "The Relation between Structure and Mechanical Properties of Metals" (Her Majesty's Stationary Office, London, 1963) p. 261.
22. W. G. JOHNSTON, *J. Appl. Phys.* **33** (1962) 2050.
23. M. SRINIVASAN and T. G. STOEBE, *J. Mater. Sci.* **9** (1974) 121.
24. J. FRIEDEL, "Dislocations" (Pergamon Press, Oxford, 1964) p. 224.
25. Y. KOHZUKI and T. OHGAKU, *J. Mater. Sci.* (in press).
26. T. OHGAKU and N. TAKEUCHI, *Phys. Status Solidi* (a) **111** (1989) 165.
27. *Idem.*, *ibid.* **118** (1990) 153.
28. Y. KOHZUKI, T. OHGAKU and N. TAKEUCHI, *J. Mater. Sci.* **28** (1993) 6329.
29. A. J. E. FOREMAN and M. J. MAKIN, *Philos. Mag.* **14** (1966) 911.
30. S. HART, *Brit. J. Appl. Phys.* (*J. Phys. D*) ser. 2 **1** (1968) 1285.
31. M. T. SPRACKLING, "The Plastic Deformation of Simple Ionic Crystals," edited by A. M. Alper, J. L. Margrave and A. S. Nowick (Academic Press, London, 1976) p. 141.
32. Y. KOHZUKI, *J. Mater. Sci.* **35** (2000) 3397.
33. K. SUMINO, *Jpn. Inst. Metals* **10** (1971) 758 (in Japanese).
34. Y. KOHZUKI, T. OHGAKU and N. TAKEUCHI, *J. Mater. Sci.* **30** (1995) 101.

Received 28 March
and accepted 5 August 2003